Available online at www.sciencedirect.com
SCIENCE DIRECT
Catalysis Today 109 (2005) 76–92
CATALYSIS TODAY
www.elsevier.com/locate/cattod

Kinetic modeling of hydrocracking of heavy oil fractions: A review

Jorge Ancheyta [a,c,*], Sergio Sánchez [a], Miguel A. Rodríguez [b]

[a] Instituto Mexicano del Petróleo, Col. San Bartolo Atepehuacan, Eje Central Lázaro Cárdenas 152, México D.F. 07730, Mexico
[b] Facultad de Ingeniería, UNAM, Ciudad Universitaria, México D.F. 04510, Mexico
[c] Escuela Superior de Ingeniería Química e Industrias Extractivas (ESIQIE-IPN), UPALM, Zacatenco, México D.F. 07738, Mexico

Abstract

An exhaustive review of the scientific literature on kinetic modeling of heavy petroleum fraction hydrocracking is reported in this paper. Kinetic models for hydrocracking of model compounds were not analyzed. The review includes models based on the lumping technique, continuous mixtures, structure oriented lumping, and single event models. Experimental data, reaction networks, main characteristics of kinetic approaches, and kinetic parameter values are also reported. In some cases when detailed experimental data were available, kinetic parameters were re-estimated and some differences were found in comparison with original reported values. One representative model of each kinetic approach was selected, and parameter estimation was done with reported experimental values in order to establish the capability and accuracy in the prediction of conversion and product yields. Advantages and disadvantages of the models are discussed in terms of their capability to predict detailed product composition, difficulty for parameter estimation, dependency of rate coefficient with feed properties, and required experimental data.

Keywords: Hydrocracking; Heavy oil; Kinetics

1. Introduction

The growing demand for middle distillates and the increasing production of heavy crude oils have placed hydrocracking as one of the most important secondary petroleum refinery processes. Hydrocracking is commonly practiced in the petroleum refining industry to treat oil residua. During hydrocracking, large compounds are broken to form low molecular weight compounds. When the reaction takes place over a catalyst in a hydrogen-rich atmosphere, other reactions, such as hydrodesulfurization, hydrodemetallization, etc., occur simultaneously. The different rates and selectivity of each reaction depend on the properties of the catalyst used and on the reaction severity. Most of the industrial processes employ catalysts with both hydrogenation and acid functions [1]; isomerization and cracking occur on acid sites via ion carbenium chemistry, whereas hydrogenation and dehydrogenation reactions take place on the metallic sites.

Various technologies are available for upgrading heavy oils. Commercial hydrocracking processes mainly use two types of reactors: fixed trickle-bed reactor (TBR) and ebullated bed reactor (EBR). In both cases, when processing heavy oils, three phases are present. The advantages of using fixed-bed reactors are the relative simplicity of scale-up and operation; the reactors operate in downflow mode, with liquid and gas (mainly hydrogen) flowing down over the catalytic bed. The major problem with this type of reactor is the accumulation of metals and coke in the mouth of the catalytic pores, blocking the access of reactants to the internal surface. The ebullated bed reactors eliminate this difficulty by fluidizing the catalyst. Metals are deposited in the catalyst inventory allowing for uniform deactivation. The catalyst is continuously added and removed in order to keep the catalytic activity at a certain constant level. In general, ebullated bed technology is most applicable for highly exothermic reactions and for feedstocks that are difficult to process in a fixed-bed reactor due to high levels of contaminants.

The design of both TBR and EBR is considerably more complicated than that of a fixed-bed gas reactor. Oil companies have developed, and are using, their own design procedures,

* Corresponding author. Tel.: +52 55 9175 8443; fax: +52 55 9175 8429.
E-mail address: jancheyt@imp.mx (J. Ancheyta).

0920-5861/$ – see front matter © 2005 Elsevier B.V. All rights reserved.
doi:10.1016/j.cattod.2005.08.015

Nomenclature

A	pre-exponential factor
a, b, c	power terms for temperature, hydrogen partial pressure, and LHSV, Eq. (1)
a, b, c, d, n	parameters of Eq. (9)
a_0, a_1, δ, A, B, D, So	model parameters of Eqs. (25) to (28)
$C(k,t)$	concentration function according to Eq. (24)
C_{HGO}	concentration of heavy gas oil (wt.%)
C_{LGO}	concentration of light gas oil (wt.%)
$D(k)$	species-type distribution function, Eqs. (23), (24) and (28)
erf	error function
E_A	activation energy (kcal/mol)
f	fraction of material in product which boils below the specified temperature
FBP_f	feed final boiling point (°C)
g	gas yield (wt.%)
I	inhibitor content (wt.%)
k', k''	kinetic factors in Eqs. (5) and (6)
k_{365}	kinetic constant with average boiling point of 365 °C (m^6_L/m^6_{cat} kmol s)
k_{50}	decay constant (h^{-1}) in Eqs. (13), (15) and (17)
k_H	overall rate constant according to Eq. (8) ($kg_{feed}/m^3_{cat}/s$)
k_{HT}, k_{HC}	apparent rate constants for hydrotreating and hydrocracking reactions in Eq. (10) ($kg_{feed}/m^3_{cat}/s$)
k_i	reaction rate constant
k_{max}	rate constant of species with the highest TBP, Eqs. (22)–(24)
LHSV	liquid hourly space velocity (h^{-1})
n	decay order in Eqs. (15) and (16)
N	total number of species, Eq. (23)
$p(k, K)$	yield distribution function, Eqs. (24) and (25)
P	paraffin content in feed (wt.%)
PA	content of polycyclic aromatics compounds (wt.%)
Pe	Peclet number for axial-dispersion model
P_{H_2}	hydrogen partial pressure (MPa)
s_i	stoichiometric coefficient
S	sulfur content (wt.%)
SV	space velocity ($kg_{feed}/m^3_{cat}/s$)
t	time
T	temperature
T^*	normalized dimensionless temperature according to Eq. (11)
T_{50}	mid boiling temperature (°F)
$T_{50,f}$	mid boiling temperature of feed (°C)
$T_{50,\tau}$	mid boiling temperature of feed affected by decay function (°C)
TBP	true boiling point (°C)
x	yield of gasoline (wt.%)
y_i	product yield (wt.%)
Y	total liquid product yield, Eq. (1) (m^3/m^3 of feed)
Y_0	Eq. (1) constant
z	diesel yield (wt.%)

Greek symbols

α	rate constant (h^{-1}) in Eq. (4); model parameter in Eqs. (22) and (23)
β	inhibition factor in Eq. (4)
τ	space time (h)
θ	index for normalized TBP in Eqs. (21) and (22)

which are not available in the public literature and are kept secret. What is not a secret is that most of the time the design is done with models and correlations supported by previous experimental and commercial experiences.

Another manner of performing the reactor design is with the use of kinetic and reactor modeling. These tools are not only utilized for this purpose but also for process simulation and optimization. Reactor modeling has been the subject of several books and papers, in which different levels of sophistication are employed, and they are already described with sufficient detail [2]. For this reason, this topic is not covered in the scope of the present work.

Kinetic modeling of hydrocracking with different approaches has also been reported in the literature. Kinetic studies considering each compound and all the possible reactions are complex due the huge number of hydrocarbons involved. However, they permit a mechanistic description of hydrocracking based on the detailed knowledge of the mechanism of the different reactions. Most of the times, applying this method to hydrocracking of real feeds is difficult because of analytical complexity and computational limitations. The situation is clear: the more compounds a model includes intrinsically the more kinetic parameters that need to be estimated; consequently, more experimental information is required.

One way to simplify the problem is to consider the partition of the species into a few equivalent classes, the so-called lumps or lumping technique, and then assume each class is an independent entity [3]. These two approaches are very well-known as being the two extreme cases for kinetic modeling of complex mixtures. The second approach is the most used nowadays due to its simplicity. There are other models which can be considered as a combination of these two methods; of course, their complexity is based on the available experimental information.

Various reviews on hydrocracking technology have been reported in the literature. Probably the first complete review was done by Choudhary and Saraf [4] in 1975. Different aspects of hydrocracking were discussed, such as types of hydrocracking, catalysis, effects of feed, catalyst acidity, pore diffusion, and catalyst poisons on hydrocracking reactions. Some of the general points of distinction among the major hydrocracking processes were also discussed. In this review, nothing was mentioned about the kinetic modeling of hydrocracking.

Mohanty et al. [5] reviewed the technology, chemistry, catalysts, kinetics, and reactor modeling of hydrocracking.

Neither kinetic models nor reactor modeling were described with enough detail, since the authors only summarized the main characteristics of the reported models. They recognized that considerable information has been published on the hydrocracking of pure hydrocarbons, in contrast with the very few reported studies on kinetics and reactor modeling of petroleum fractions hydrocracking.

Chaudhuri et al. [6] discussed the state-of-the-art of mild hydrocracking processes, including data characterization reactivities, reaction networks, and kinetics. Comparisons were made between hydrocracking and mild hydrocracking. Only a few kinetic models for hydrocracking were mentioned. These authors concluded that the complexity of the industrial feedstocks suggests that the use of pseudocomponents would continue in the study of reaction kinetics.

The most recent review of hydrocracking has been reported by Valavarasu et al. [7], who focused their contribution on important aspects of mild hydrocracking, such as processes, catalysts, reactions, and kinetics. These authors also emphasized that the available literature on the kinetics of hydrocracking is scarce, and that structural modeling based on complete hydrocarbon structures needs to be studied in detail.

Although several reviews on hydrocracking have been published, kinetic aspects when hydrocracking real feeds have not received too much attention. Hence, the subject of the present contribution is the description, analysis, and application of the main kinetic models for hydrocracking of oil fractions reported in the literature up to date. The scope of this work is limited to those models based on hydrocracking experimental data obtained with heavy oil fractions.

2. Kinetic models

To better organize this review, the models have been classified as: (1) models based on lumping technique, (2) models based on continuous mixtures, and (3) structure oriented lumping and single event models.

2.1. Traditional lumping

2.1.1. Models based on wide distillation range fractions

The kinetics of hydrocracking of gas oil was studied by Qader and Hill [8], in a continuous fixed-bed tubular flow reactor. These authors found that the rate of hydrocracking is of first order with respect to feed concentration (Fig. 1a), with an activation energy of 21.1 kcal/mol. The kinetic data were obtained at 10.34 MPa pressure, 400–500 °C temperature, 0.5–3.0 h^{-1} space velocity, and a constant H_2/oil ratio of 500 Std m^3/m^3. The liquid product was distilled into gasoline (IBP-200 °C), middle distillate (200–300°C), and diesel (300 °C+). This seems to be the first experimental study in which kinetics of hydrocracking of real feed is reported.

Callejas and Martínez [9] studied the kinetics of Maya residue hydrocracking. They used a first-order kinetic scheme involving three-lump species: AR, atmospheric residuum (343 °C+); LO, light oils (343 °C−); gases (Fig. 1b). The

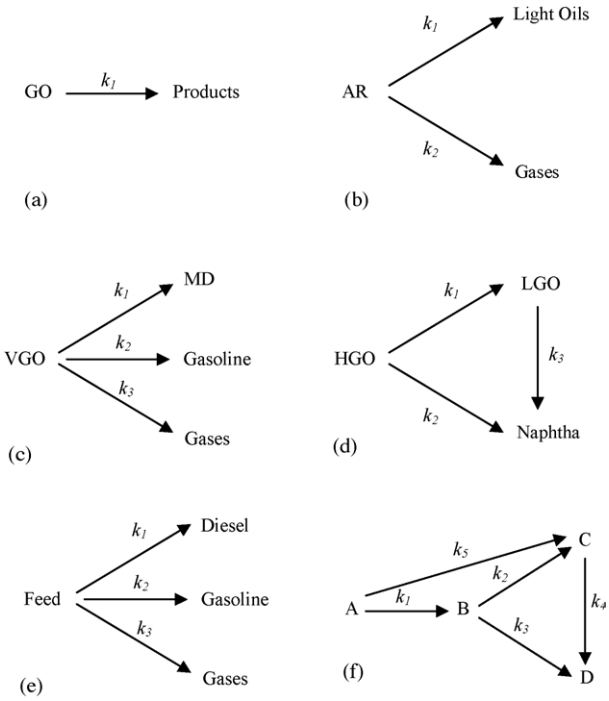

Fig. 1. Reaction schemes for hydrocracking lump-kinetic models.

experiments were conducted continuously in a stirred tank reactor (1 L) in the presence of a NiMo catalyst supported on γ-Al_2O_3. All tests were carried out at 12.5 MPa of hydrogen pressure at temperatures of 375, 400, and 415 °C, and WHSV in the range of 1.4–7.1 L/g_{cat} h. The total liquid products from each experiment were analyzed by simulated distillation using the ASTM D-2887 method, which was employed to estimate the boiling distribution of the oil samples. The rate constants at different temperatures are listed in Table 1. The authors reported that experimental data at 375 and 400 °C are in agreement with the proposed model ($r > 0.82$), but at 415 °C, the fits were bad ($r < 0.70$).

Fortunately, these authors reported the detailed experimental data that they used for kinetic parameter calculation, thus allowing us to re-calculate them for the purposes of this work. The first concern to arise was the fact that by definition, the sum of k_1 and k_2 must be equal to k_0, and, as can be seen in Table 1, this does not happen in the original reported k_i values estimated

Table 1
Rate constants [L/g_{cat}h] for the hydrocracking of Maya AR according to Fig. 1b

	375 °C	400 °C	415 °C	E_A (kcal/mol)
k_0 (AR conversion)				
Original value [9]	1.13	3.26	9.20	45.32
This work	1.09	3.18	7.22	41.32
k_1 (Light oils formation)				
Original value [9]	0.07	0.25	1.52	64.40
This work	0.30	0.46	1.45	32.57
k_2 (Gases formation from AR)				
Original value [9]	0.21	1.5	5.12	70.43
This work	0.79	2.72	5.77	43.90

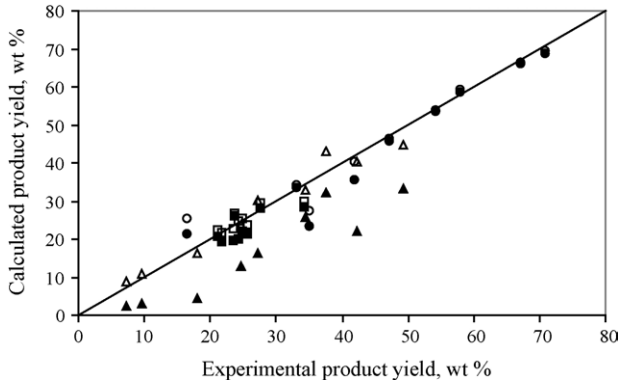

Fig. 2. Comparison of experimental data and results obtained with kinetic parameters reported by Callejas and Martinez [9] (full symbols) and those obtained in this work (void symbols): (○, ●) atmospheric residuum; (□, ■) light oils; (△, ▲) gases.

by lineal regression. At the beginning it appeared to be an editing problem, but the same occurs with the three temperatures. This inconsistency is due to the individual estimation of k_1, k_2, and k_0 by lineal regression. Our k_i values, determined by minimization of the sum of square errors (SSE) between experimental and calculated yields, do satisfy this condition ($k_0 = k_1 + k_2$), and the SSE was lower than that obtained with Callejas and Martínez's [9] kinetic parameters. A comparison of predicted and experimental yields using original kinetics parameters values and those determined in this work is presented in Fig. 2, in which can be clearly seen the better fit obtained with our optimized k_i values, especially for gases lump. Activation energies were calculated and are also reported in Table 1. It is observed that parameter estimation by lineal regression gives higher values than nonlinear regression. Of course, the second approach is more accurate.

Aboul-Gheit [10] determined the kinetic parameters of vacuum gas oil (VGO) hydrocracking, expressing composition in molar concentration. The experiments were carried out at 400, 425, and 450 °C, 0.5–2 h^{-1} LHSV, and 12 MPa pressure. Two different NiMo catalysts with HY zeolite supported on a silica–alumina matrix were used. He proposed that VGO reacts to form gases, gasoline, and middle distillates (MD) according to the reaction scheme shown in Fig. 1c. Kinetic parameters and activation energies are summarized in Table 2. The same problem as in the previous model was observed. In this case, the sum of the reported values of k_1, k_2, and k_3 does not correspond to k_0, which is also due to the individual determination of each parameter by lineal regression. The exact values of k_0 are reported within parentheses in Table 2, and they are very close to the original values. Consequently, the activation energies determined with the two series of k_0 values are also similar.

Another kinetic model for gas oil hydrocracking was proposed by Yui and Sanford [11], who performed experiments in a pilot plant with a trickle-bed reactor at different operating conditions (350–400 °C, 7–11 MPa, 0.7–1.5 h^{-1} LHSV, and H_2/oil ratio of 600 Std m^3/m^3). They used Athabasca bitumen-derived coker and hydrocracker heavy gas oils (HGO) as feed and two different commercial NiMo/Al_2O_3 hydrotreating catalysts. A three-lump model was considered (HGO, heavy gas oil; LGO, light gas oil; naphtha), which can follow parallel, consecutive, and combined reaction schemes as shown in Fig. 1d. The model includes first-order reactions and considers the effects of partial pressure (in MPa), temperature (in °C), and space velocity on the total liquid products yield [Eq. (1)]. Fitted parameters are $Y_0 = 1.0505$, $a = 0.2517$, $b = 0.0414$, and $c = -0.0163$ for the coker gas oil; $Y_0 = 1.0371$, $a = 0.1133$, $b = 0.0206$, and $c = -0.0134$ for the hydrocracker gas oil. The kinetic parameters are presented in Table 3. According to the authors, it was not possible to fit a set of parameters for the combined reaction scheme:

$$Y = Y_0\left(\frac{T}{400}\right)^a\left(\frac{P_{H_2}}{10}\right)^b \mathrm{LHSV}^c \quad (1)$$

$$\frac{dC_{HGO}}{d(1/LHSV)} = -(k_1 + k_2)C_{HGO} \quad (2)$$

$$\frac{dC_{LGO}}{d(1/LHSV)} = k_1 C_{HGO} - k_3 C_{LGO} \quad (3)$$

The kinetics of hydrocracking of vacuum distillates from Romashkin and Arlan crude oils was studied by Orochko [12] in a fixed-bed reactor over an alumina–cobalt molybdenum catalyst using a first-order kinetic scheme involving four lumps, according to the scheme shown in Fig. 1e. This model is similar to that proposed by Aboul-Gheit [10] (Fig. 1c). The rate of a

Table 2
First-order rate constants and activation energies obtained by Aboul-Gheit [10]

	Catalyst 1				Catalyst 2			
	Temperature (°C)			E_A (kcal/mol)	Temperature (°C)			E_A (kcal/mol)
	400	425	450		400	425	450	
k_1 (h^{-1})	0.286	0.500	0.688	17.51	0.469	0.612	0.916	13.09
k_2 (h^{-1})	0.040	0.083	0.140	24.02	0.111	0.216	0.350	22.23
k_3 (h^{-1})	0.026	0.048	0.069	18.67	0.040	0.074	0.106	18.96
k_0[a] (h^{-1})	0.352	0.631	0.897	18.14	0.620	0.902	1.372	15.35
	(0.333)	(0.667)	(1.059)	22.51	(0.714)	(1.125)	(1.75)	17.15

[a] Values in parentheses correspond to $k_1 + k_2 + k_3$.

Table 3
Kinetic parameters reported by Yui and Sanford [11]

	Coker feed		Hydrocracker feed	
	A (h^{-1})	E_A (kcal/mol)	A (h^{-1})	E_A (kcal/mol)
Parallel scheme ($k_3 = 0$)				
HGO $\xrightarrow{k_1}$ LGO				
HGO $\xrightarrow{k_2}$ Naphtha				
$k_1 + k_2$	8.754×10^4	17.75	4.274×10^4	17.24
k_1	8.544×10^3	15.02	3.775×10^3	14.32
k_2	1.780×10^8	29.78	6.847×10^8	32.17
Consecutive scheme ($k_2 = 0$)				
HGO $\xrightarrow{k_1}$ LGO $\xrightarrow{k_3}$ Naphtha				
k_1	8.754×10^4	17.75	4.274×10^4	17.24
k_3	6.206×10^7	26.96	2.711×10^5	20.46
Combined scheme				
It was not possible to fit the data				

first-order heterogeneous catalytic reaction was expressed by the following equation:

$$\alpha\tau = \ln\frac{1}{1-y} - \beta y \tag{4}$$

where α is the rate constant, τ the nominal reaction time, y the total conversion, and β is the inhibition factor of the process by the reaction products formed and absorbed on the active surface of the catalyst and also by their effect on the mass transfer in the heterogeneous process. These authors indicate that in this case the consecutive reactions predominate, the parallel reactions in the calculations being comparatively minor and negligible to a first approximation. All experiments were carried out at 5 and 10.13 MPa of hydrogen pressure and temperatures of 400, 425, and 450 °C. For the case of Arlan petroleum vacuum distillate at 425 °C and 10.13 MPa, a value of $\beta = 1$ was reported. Rate constants and activation energies based on the experimental data reported by others [13] are given in Table 4. For the case of Romashkin petroleum vacuum distillates, two values of E_A were calculated at each pressure, each one with two values of temperature. Re-calculated activation energies with all temperatures for each pressure, which are in between those originally reported, are also given in Table 4. The kinetic equations assume the following form:

- Diesel fraction yield:

$$z = \frac{(1-y)^{k'} - (1-y)}{1-k'} \tag{5}$$

- Gasoline yield:

$$x = k'\frac{(1-y)^{k''} - (1-y)^{k'}}{(1-k')(k'-k'')} + k'\frac{(1-y) - (1-y)^{k''}}{(1-k')(1-k'')} \tag{6}$$

- Gases yield:

$$g = y - (z + x) \tag{7}$$

where k' and k'' are kinetic factors with similar meaning to the rate constants, which are determined from the experimental data, and are dependent on the equivalent kinetic temperature of the process and the catalyst activity. For the Romashkin petroleum vacuum distillate at 10.13 MPa, the values of k' and k'' are 1.3 and 2.0, respectively.

Botchwey et al. [14] studied overall conversion kinetic models within specified, short-ranged temperature regimes for the hydrotreating of bitumen-derived heavy gas oil from Athabasca over a commercial $NiMo/Al_2O_3$ catalyst in a trickle-bed reactor. All experiments were carried out at various reaction temperatures between 340 and 420 °C, 8.8 MPa of pressure, LHSV of 1 h^{-1}, and a H_2/oil ratio of 600 Std m^3/m^3.

The oil samples (feed and products) were grouped into four different boiling cuts with temperature ranges of: D (IBP-300 °C), C (300–400 °C), B (400–500 °C), and A (500–600 °C). The boiling point distribution was derived from GC simulated distillation. It should be noted that the product analyses were limited to liquid samples, because negligible amounts of gaseous hydrocarbon products were formed from mass balances.

Fig. 1f shows the proposed kinetic model which includes the four lumps (A, B, C, and D), and five kinetic parameters ($k_1, \ldots, k_5$). The low severity temperature regime was considered to be

Table 4
Rate constants for the hydrocracking reactions reported by Orochko [12]

Feedstock	Temperature (°C)	Total pressure (MPa)	Rate constant, α	Apparent activation energy E_A (kcal/mol)	
Romashkin petroleum vacuum distillate	400	5.06	0.040	60.0	56.7
	425	5.06	0.200	53.2	
	450	5.06	0.750		
	400	10.13	0.046	61.8	63.8
	425	10.13	0.240	66.6	
	450	10.13	1.250		
Arlan petroleum vacuum distillate	400	5.06	0.050		
	425	5.06	0.270	63.0	
	400	10.13	0.060		
	425	10.13	0.800 (0.30)[a]	64.8	

[a] With $\alpha = 0.8$, E_A is different to the reported value of 64.8 kcal/mol. The correct value of α is that given in parenthesis.

Table 5
First-order apparent kinetic parameters for overall conversion of high-boiling species to low-boiling products oil at 8.8 MPa, LHSV of 1 h^{-1} and hydrogen-to-oil ratio of 600 m^3/m^3

	k_1	k_2	k_3	k_4	k_5
Low severity temperature regime (340–370 °C)					
340	0.064	0.016	0.147	–	–
350	0.100	0.032	0.163	–	–
360	0.164	0.053	0.184	–	–
370	0.229	0.076	0.207	–	–
E_A (kcal/mol)	33.94	40.15	8.84	–	–
ln[A]	25.2	28.9	5.4	–	–
R^2	0.996	0.986	0.997	–	–
Intermediate severity temperature regime (370–400 °C)					
370	0.229	0.116	0.167	0.050	–
380	0.299	0.148	0.199	0.070	–
390	0.393	0.186	0.237	0.101	–
400	0.531	0.242	0.293	0.151	–
E_A (kcal/mol)	24.14	21.03	16.01	31.79	–
ln[A]	17.3	14.2	10.7	21.9	–
R^2	0.998	0.999	0.996	0.997	–
High severity temperature regime (400–420 °C)					
400	0.195	0.201	0.252	0.151	0.169
410	0.259	0.276	0.327	0.220	0.233
420	0.334	0.357	0.408	0.293	0.308
E_A (kcal/mol)	25.57	26.53	22.46	29.16	28.44
ln[A]	17.9	18.2	15.4	20.1	19.9
R^2	0.999	0.997	0.998	0.983	0.999

that at the lowest operating temperature range (340–370 °C), and the reactions *A* to *C* and *C* to *D* were negligible. In the intermediate severity temperature regime (370–400 °C), only the reaction *A* to *C* was negligible. The value of k_5 is equal to zero in both kinetic schemes derived from both temperature regimes. The high severity temperature regime covered the most severe operating temperature range (400–420 °C). All kinetic parameter values for the three regimes are tabulated in Table 5.

Another reaction pathway was proposed by Botchwey et al. [15] and is shown in Fig. 3. The pathways describe the conversion of gas oil to products via heteroatom removal, aromatics saturation, and hydrocracking. Typical hydrotreating reactions are represented by solid lines, while cracking reactions are shown as dashed lines. These authors consider conversion to take place according to different regimes, namely, the hydrotreating regime (reactions 1–7) at temperatures of 340–390 °C and the mild hydrocracking regime (reactions 1–9) at 390–420 °C. They arrived at this conclusion after performing experiments in a trickle-bed micro reactor. The study covered a pressure range between 6.5 and 11 MPa, at temperatures of 360, 380, and 400 °C. The liquid hourly space velocity and the H_2/oil ratio were maintained constant at 1 h^{-1} and 600 Std m^3/m^3 respectively. However, kinetic expressions and rate constants are not given.

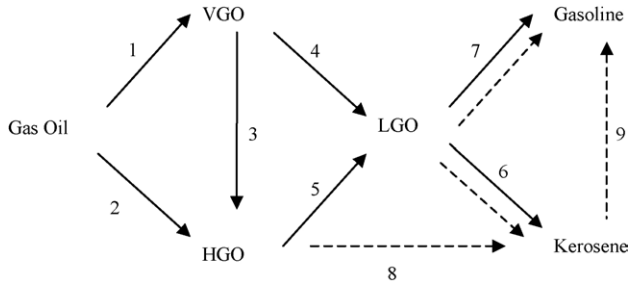

Fig. 3. Reaction network proposed by Botchwey et al. [15].

Aoyagi et al. [16] studied the kinetics of hydrotreating and hydrocracking of conventional gas oils, coker gas oils, and gas oils derived from Athabasca bitumen. They were interested in studying the influence of feed properties on product yield and composition. The experiments were fixed as follows: a temperature of 380 °C, an operating pressure at 13.8 MPa, a liquid hourly space velocity of 0.75 h^{-1}, and a H_2/oil ratio of 400 Std m^3/m^3. The feeds with different properties were obtained mixing hydrotreated gas oils with gas oil without hydrotreating. A kinetic model was developed and the parameters were adjusted with experimental data from a system with two reactors in series, each one with a different catalyst. In the first reactor, a commercial NiMo/γ-Al_2O_3 catalyst was used, and in the second reactor, a commercial hydrocracking catalyst with NiMo/boria USY was employed. The model considers that in the first hydrotreating reactor the modifications in molecular weight are due to reactions of hydrodesulfurization and hydrogenation of polycyclic aromatic compounds. Hydrocracking is the most important reaction in the second reactor. A very simplified scheme of the kinetic model is presented in Fig. 4.

The model uses a first-order expression to describe the rate of disappearance of heavy gas oil (HGO), given by Eq. (8), where k_H is the overall hydrocracking rate constant. Its value depends on both hydrotreating and hydrocracking reactions and is calculated with Eq. (9), in which the last term includes the nitrogen content's inhibitor effect. HGO_{in} and HGO_{out} are the inlet and outlet concentrations of heavy gas oil; [S], [PA], and [I] are the contents of sulfur, polycyclic aromatics compounds, and inhibitors. The best set of model parameters reported by the authors is: $a = 9.5 \times 10^{-4}$, $b = 1.8 \times 10^{-3}$, $c = 0.32$, $d = 9.1 \times 10^{-4}$, and $n = 2$:

$$C_{HGO_{out}} = C_{HGO_{in}} \exp\left(-\frac{k_H}{SV}\right) \quad (8)$$

$$k_H = a[S] + b[PA] + c(1 + d[I])^{-n} \quad (9)$$

$$k_H = k_{HT} + k_{HC} \quad (10)$$

Mosby et al. [17] reported a model to describe the performance of a residue hydrotreater using lumped first-order kinetics. Fig. 5 shows the proposed model, which divides residue into lumps that are "easy" and "hard" to crack. This

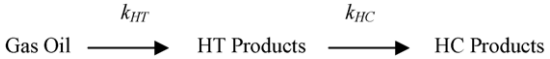

Fig. 4. Simplified scheme of the kinetic model proposed by Aoyagi et al. [16].

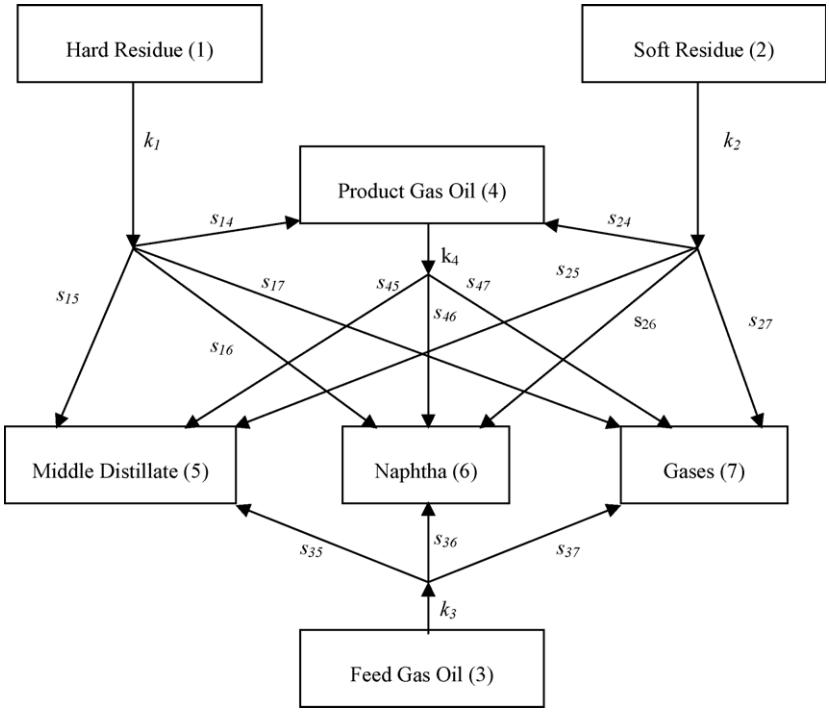

Fig. 5. Generalized lumped kinetic model for hydrocracking of residues proposed by Mosby et al. [17].

lumping scheme was used by Ayasse et al. [18] to fit experimental product yields from catalytic hydrocracking of Athabasca bitumen obtained in a continuous-flow mixed reactor over a NiMo catalyst at 430 °C and 13.7 MPa. To develop the model, stoichiometry concepts of a complex reacting mixture were applied. The resulting compact model was fitted to data from single-pass hydrocracking and used to predict the performance of multi-pass experiments. The liquid product was distilled into four cuts: naphtha (IBP-195 °C), middle distillates (195–343 °C), gas oil (343–524 °C), and residue (>524 °C). Residue fraction was then distilled under vacuum to obtain the gas oil and residue fractions, using the ASTM D1160 procedure.

After all the data had been utilized to estimate the parameters of the general lumped model shown in Fig. 5, it was found that the model was over-determined, as is illustrated in Fig. 6a. The number of parameters was too large, and it was concluded that seven lumps are not required to give the experimental data a satisfactory fit.

Afterward, three new models were proposed, two with six lumped components and one with five lumps, which were considered to be adequate to describe the data with an equivalent sum of squared residuals. In Model 1, hard and soft residues were lumped as a single component under ‘‘hard residue’’. The initial concentration of lump 2 was zero, and the kinetic parameters of this lump (k_2, s_{24}, s_{25}, s_{26}, and s_{27}) were not determined. In Model 2, all the gas oil, whether it originated with the feed or was formed by cracking of the residue, was lumped as a single component under ‘‘product gas oil’’. The initial concentration of lump 3 was zero, and the kinetic parameters of this lump (k_3, s_{35}, s_{36}, and s_{37}) were not determined. Consequently, the simplest model that could capture this chemistry was a five-lump model (Model 3),

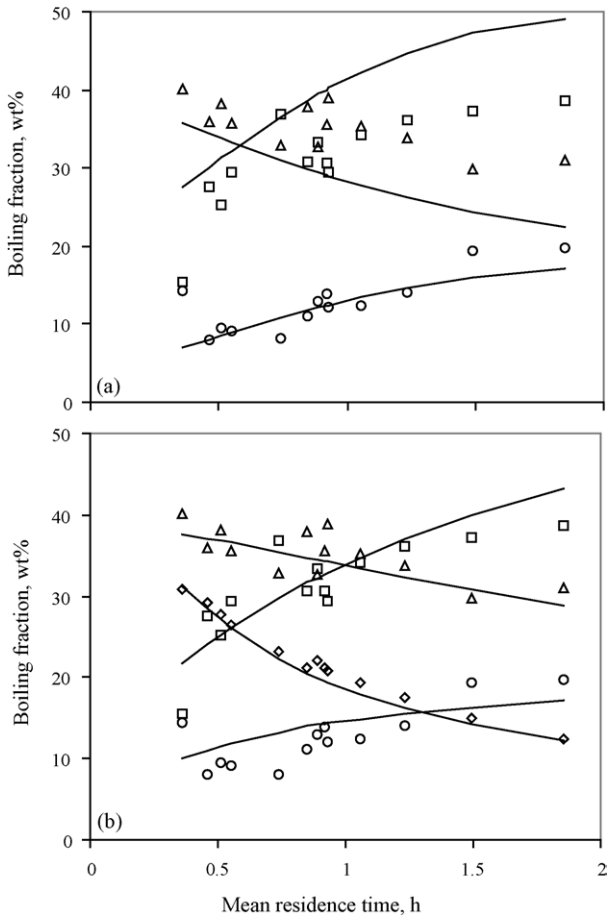

Fig. 6. Yields from single-pass catalytic hydrocracking of Athabasca bitumen as function of mean residence time. The lines are best fit to (a) model of Mosby et al. [17], (b) Model 1 using the parameters given in Table 6: (○) naphtha; (□) middle distillates; (△) gas oil, (◇) residue.

Table 6
Kinetic parameters reported by Ayasse et al. [18]

Data fitted	Model 1, two gas oils, all data sets	Model 2, two residues, Bitumen-feed data sets	Model 3, five lumps, multi-pass data sets	Model 3, five lumps, all data sets
Number of lumps	6	6	5	5
Stoichiometric coefficients				
Hard residue				
To gas oil (s_{14})	0.86	0.21	0.15	0.1
To middle distillates (s_{15})	0.14	0.79	0.45	0.55
To naphtha (s_{16})	0	0	0.31	0.34
To gas (s_{17})	0	0	0.09	0
Soft residue				
To gas oil (s_{24})	–	0.11	–	–
To middle distillates (s_{25})	–	0	–	–
To naphtha (s_{26})	–	0.89	–	–
To gas (s_{27})	–	0	–	–
Feed gas oil				
To middle distillates (s_{35})	0.37	–	–	–
To naphtha (s_{36})	0.46	–	–	–
To gas (s_{37})	0.17	–	–	–
Product gas oil				
To middle distillates (s_{45})	0.74	0.47	0.04	0.05
To naphtha (s_{46})	0	0.53	0	0
To gas (s_{47})	0.26	0	0.96	0.95
Rate constants (h^{-1})				
Hard residue (k_1)	2.2	1.3	2.5	2.4
Soft residue (k_2)	–	19	–	–
Feed gas oil (k_3)	3	–	–	–
Product gas oil (k_4)	0.48	0.41	0.49	0.34
Fraction of hard residue (f_H)	–	0.76	–	–
Sum of squared residuals	1.72×10^4	2.01×10^4	3.26×10^4	2.56×10^4

consisting of one residue lump (hard residue), one gas oil lump (product gas oil), middle distillates, naphtha, and light ends. The resulting five-lump model had seven independent parameters (two rate constants and five independent stoichiometric coefficients).

Data from all the experiments were then used to determine the optimal parameter values, which are listed in Table 6. The results in Fig. 6b show that Model 1 over-predicted the yield of middle distillates and underestimated the yield of naphtha at high residue conversion in experiments with bitumen as feed. Model 1 was therefore satisfactory for fitting yields over a wide range of residue conversion. Model 2 was inferior to Model 1 in predicting the products, with large errors in the proportions of naphtha (+4.6%) and gas oil (−5.1%). However, Model 3 underestimated the yield of middle distillates and tended to over-predict the yield of gas oil. The models with six and seven lumps are unnecessarily complex for these data, whereas the simpler five-lump model is satisfactory.

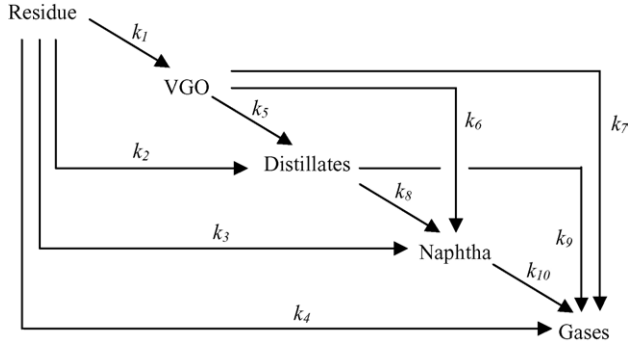

Fig. 7. Five-lump kinetic model proposed by Sánchez et al. [19].

Recently, Sánchez et al. [19] proposed a five-lump kinetic model for moderate hydrocracking of heavy oils (Fig. 7): (1) unconverted residue (538 °C+), (2) vacuum gas oil (VGO: 343–538 °C), (3) distillates (204–343 °C), (4) naphtha (IBP-204 °C), and (5) gases. The model includes 10 kinetic parameters which were estimated from experimental data obtained in a fixed-bed down-flow reactor, with Maya Heavy Crude and a NiMo/γ-Al_2O_3 catalyst at 380–420 °C reaction temperature, 0.33–1.5 h^{-1} LHSV, H_2-to-oil ratio of 890 m^3/m^3, and 6.9 MPa pressure. Kinetic parameter values are reported in Table 7. The kinetic model was developed for basic reactor modeling studies of a process for hydrotreating of heavy petroleum oils which, among several characteristics, operates at moderate reaction conditions and improves the quality of the feed while keeping the conversion level low.

2.1.2. Models based on pseudocomponents (discrete lumping)

Krishna and Saxena [20] reported a detailed kinetic model with seven lumps in which different cut temperatures are

Table 7
Kinetic parameters of the model proposed by Sánchez et al. [19]

Kinetic parameter (h^{-1})	Temperature (°C)			Activation energy, E_A (kcal/mol)
	380	400	420	
Resid				
k_1	0.042	0.147	0.362	48.5
k_2	0.008	0.022	0.057	44.2
k_3	0.008	0.020	0.043	38.0
k_4	0.041	0.098	0.137	27.3
VGO				
k_5	0.018	0.057	0.104	39.5
k_6	0	0.007	0.016	37.1
k_7	0	0	0	–
Distillate				
k_8	0	0.003	0.010	53.7
k_9	0	0	0	–
Naphtha				
k_{10}	0	0	0	–

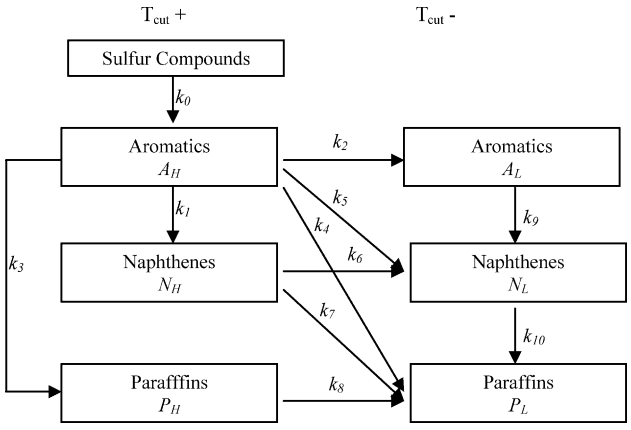

Fig. 8. Detailed lumped reaction scheme for hydrocracking proposed by Krishna and Saxena [20].

considered. The scheme of the kinetic network is shown in Fig. 8. The lumps are sulfur compounds, heavy and light aromatics, naphthenes, and paraffins. The pseudocomponents are considered light if they are formed from fractions with boiling points lower than the cut temperature (T_{cut}). Sulfur compounds are considered to be a heavy lump. Experimental data reported by Bennett and Bourne [21] were used to test the model; the values of the 60 kinetic parameters are presented in Table 8. Fig. 9 shows a comparison of predicted results with experimental data. The authors proposed a second model based on the analogy between reactions of hydrocracking and the phenomena of axial dispersion of a tracer in a flow; this other model used only two parameters.

The dispersion model is based on the study of the TBP (true boiling point) curves of hydrocracking products. An increment in residence time causes reduction of the average molecular weight of the product and a drop in the distillation curve's middle boiling point (T_{50}). A normalization of the TBP curves at different residence times to obtain values of T^* is made

Table 8
First-order rate constants for the reaction network of Fig. 8

Kinetic constants (h^{-1})	T_{cut} (°C)					
	371	225	191	149	82	0
k_0	8.3000	–	–	–	–	–
k_1	1.2633	0.4943	0.4799	0.4624	0.4345	0.4000
k_2	0.6042	0.1809	0.1105	0.0397	0.0034	0.0000
k_3	0.0421	0.3131	0.2719	0.2593	0.2501	0.2302
k_4	0.5309	0.0211	0.0096	0.0095	0.0095	0.0095
k_5	0.0397	0.0383	0.0249	0.0131	0.0086	0.0000
k_6	1.1855	0.2772	0.2134	0.1117	0.0073	0.0000
k_7	0.1619	0.0474	0.0275	0.0275	0.0275	0.0275
k_8	0.4070	0.2391	0.1993	0.1518	0.0978	0.0299
k_9	0.2909	0.5434	0.5219	0.4509	0.4391	–
k_{10}	0.0818	0.0740	0.0709	0.0618	0.0608	–

according to Eq. (11), where FBP_f is the final boiling point of the feed. Krishna and Saxena [20] used Bennett and Bourne's [21] pilot plant experimental data to develop the model. The normalized temperature data of feed and products, shown in Fig. 10, can be roughly described by Eq. (12); the solid line is the representation of the axial dispersion model where $Pe = 14$. The mid boiling point temperature is obtained with Eq. (13), which assumes a first-order decay function:

$$T^* = \frac{FBP_f - T}{FBP_f - T_{50}} \tag{11}$$

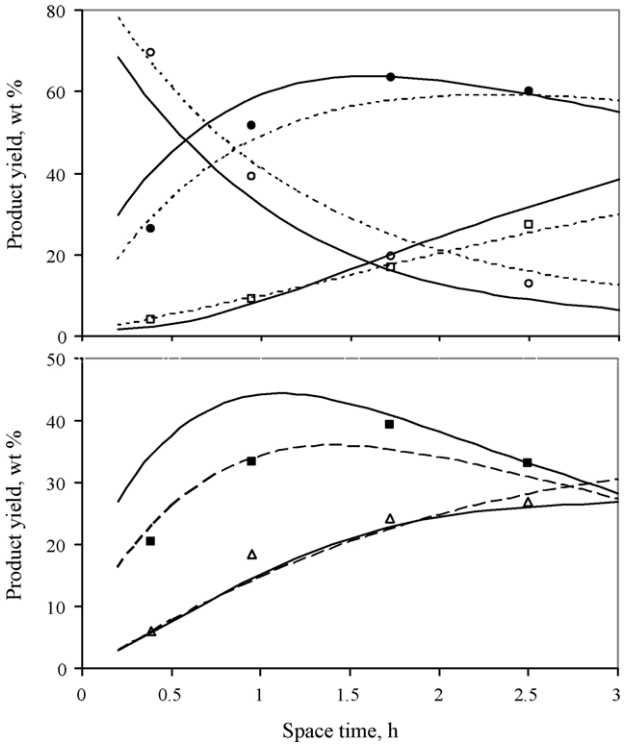

Fig. 9. Comparison of calculated yields of hydrocracking obtained by Krishna and Saxena [20] (dispersion model (—) and detailed kinetic model (- - -)) with experimental data reported by Bennett and Bourne [21]. (○) 371 °C+; (●) 149–371 °C; (□) 149 °C−; (■) 149–225 °C; (△) 225–371 °C.

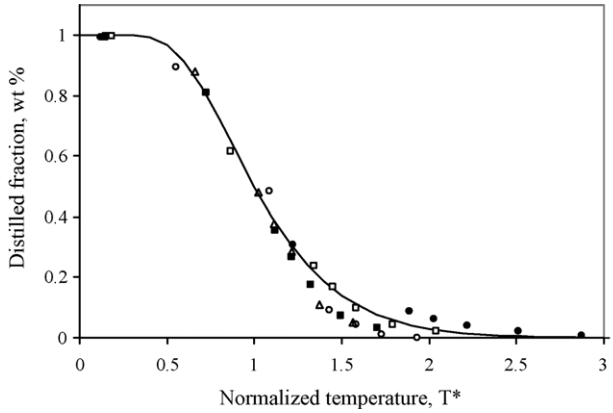

Fig. 10. Normalized TBP curves for feedstock (○) and product yields at different space times: (●) 0.383 h^{-1}; (□) 0.952 h^{-1}; (■) 1.724 h^{-1}; (△) 2.5 h^{-1}.

$$f = \frac{1}{2} + \frac{1}{2}\,\mathrm{erf}\left(\frac{1 - T^*}{(2T^*)^{0.5}} Pe^{0.5}\right) \tag{12}$$

$$T_{50,\tau} = T_{50,f}\exp(-k_{50}\tau) \tag{13}$$

Furthermore, Krishna and Saxena [20] developed empirical correlations to predict the values of decay rate of T_{50} (k_{50}) with respect to residence time (τ) and Peclet number (Pe). Both parameters are functions of the paraffin content in the feedstock (P). The following equations permit the estimation of these parameters considering an n-order decay function:

$$Pe = 20.125 - 0.175P \tag{14}$$

$$\frac{\mathrm{d}(T_{50,\tau}/T_{50,\mathrm{f}})}{\mathrm{d}\tau} = -k_{50}\left(\frac{T_{50,\tau}}{T_{50,\mathrm{f}}}\right)^n \tag{15}$$

$$n = 1.9 - 0.0015P \tag{16}$$

$$k_{50} = 0.4 - 0.003P \tag{17}$$

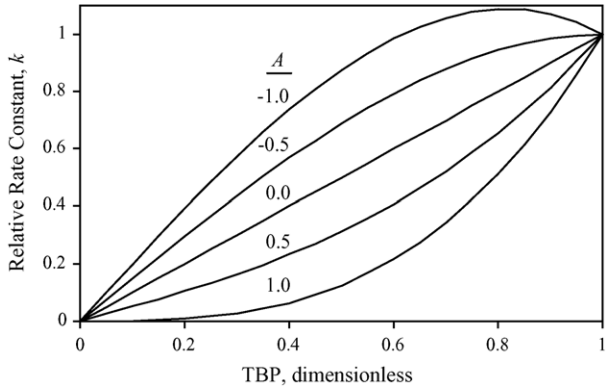

Fig. 11. Cracking rate function [22].

Stangeland [22] developed a kinetic model for predicting hydrocracker yields using correlations based on the boiling point of each of the pseudocomponents that characterize the cut. The model includes four parameters: k_0 and A quantify each pseudocomponent's reaction rate, C gives the butane yield magnitude, and B varies with both the type of feed (naphtenic or paraffinic) and the type of catalytic process (random or selective). Parameters B and C determine the shape of the yield curve. Although A usually lies in the range 0–1.0, it can take negative values. Parameter A determines the shape of the reactivity curve, which varies from a linear to a cubic function, as shown in Fig. 11. The complete set of equations, presented in Table 9, permits the calculation of the formation of component "i" due to decomposition of heavy components "j".

Sets of data at three conversion levels are illustrated in Fig. 12 for hydrocracking of raw California gas oil in once-through liquid operation. The predicted yields based upon these parameters are shown as dotted lines for conversions of 50, 73, and 92% (288 °C−). In general, the agreement with experimental data is quite good and the differences are probably within the experimental error.

The major disadvantage of this approach is that a change in the specification of the hydrocracker product, or in the number of products, requires reformulating the model and refitting the data.

Mohanty et al. [23] implemented Stangeland's kinetic model in a computer model for a two-stage commercial-scale vacuum

Table 9
Equations of the kinetic model for hydrocracking based on TBP of pseudocomponents

Model proposed by Stangeland [22]	
$\frac{\mathrm{d}}{\mathrm{d}t}F_i(t) = -k_iF_i(t) + \sum_{j=1}^{i-1}P_{ij}k_jF_j(t)$	Mass balance
$k(T) = k_0[T + A(T^3 - T)]$	Cracking rate constant function
$PC_{ij} = [y_{ij}^2 + B(y_{ij}^3 - y_{ij}^2)](1 - [C_4]_j)$	Liquid product distribution function
$[C_4]_j = C\exp[-0.00693(1.8\,\mathrm{TBP}_j - 229.5)]$	Weight fraction of butane
$y_{ij} = \frac{\mathrm{TBP}_i - 2.5}{(\mathrm{TBP}_j - 50) - 2.5}$	Normalized boiling point temperature (TBP)
$P_{ij} = PC_{ij} - PC_{i-1,j}$	Actual fraction of lighter component
Model modified by Dassori and Pacheco [24]	
$\sum_{i=1}^{j-2}P_{i,j}\mathrm{MW}_i = (\mathrm{MW}_j - n_j\mathrm{MW}_{\mathrm{H}_2})$	Mass balance for each individual reaction
$PC_{ij} = [y_{ij}^2 + B_1y_{ij}^3 - B_2y_{ij}^2](1 - [C_4]_j)$	Modified product distribution function (with B_2)
$[C_4]_j = C\exp[-\omega(1.8\,\mathrm{TBP}_j - 229.5)]$	Modified weight fraction of butane (with ω)

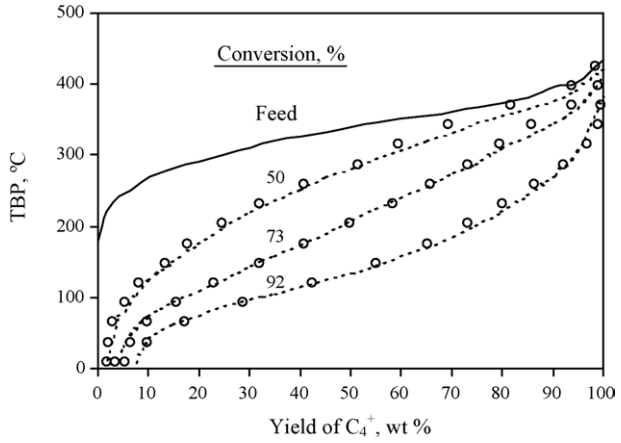

Fig. 12. Comparison of measured (○) and predicted (- - -) yields for once through hydrocracking [22].

gas oil (VGO) hydrocracker. The feed and products were lumped into 23 pseudocomponents for the hydrocracking reactions, and pseudo-homogeneous first-order reactions were assumed. Estimation of the hydrocracking kinetic constants for the other pseudocomponents that comprise the VGO was done through the following relationship:

$$k_i(T) = k_{365} K_i \tag{18}$$

where K_i was adjusted with plant data using the following functionality (Fig. 13):

$$K_i = 0.494 + 0.52 \times 10^{-2}\,\mathrm{TBP}_i - 2.185 \times 10^{-5}\,\mathrm{TBP}_i^2 + 0.312 \times 10^{-7}\,\mathrm{TBP}_i^3 \tag{19}$$

A hydrocracking kinetic constant of vacuum gas oil with an average boiling point of 365 °C reported by Qader and Hill [8] was employed:

$$k_{365} = 4.273 \times 10^3 \exp\left(\frac{-2.11 \times 10^4}{RT}\right) \tag{20}$$

Calculated yields, hydrogen consumption, and outlet temperatures with this model are tabulated in Table 10. The model was validated against plant data and the agreement was generally good. It is important to indicate that with the parameters reported by Mohanty et al. [23], the mass balance closure in each individual hydrocracking reaction is not satisfied.

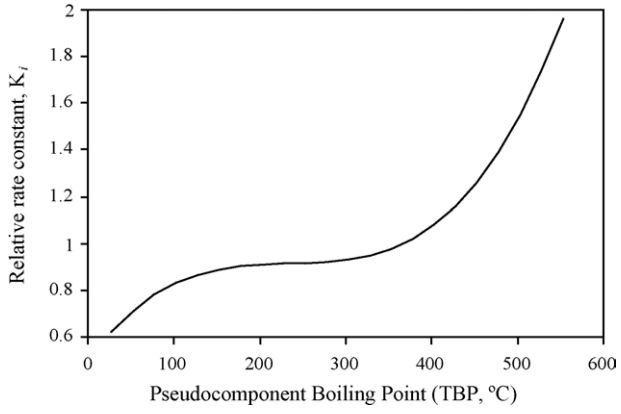

Fig. 13. Relative rate constant function [23].

Table 10
Comparison of calculated and plant data obtained by Mohanty et al. [23]

Data	Calculated results	Plant data	Error (%)
Total feed to second stage (kg/h)	183, 236	183, 385	−0.08
Hydrogen consumption (kg/h)			
First stage	2816	3267	−13.8
Second stage	1196	1363	−12.2
Reactor outlet temperature (°C)			
First stage	693.3	714 (max)	–
Second stage	677.7	700 (max)	–
High speed diesel (wt.%)	48.79	50.5	−3.46
Aviation turbine fuel (wt.%)	30.53	29.4	3.83
Naphtha (wt.%)	16.17	15.8	2.51
Butanes and lights (wt.%)	4.51	4.5	0.22

Dassori and Pacheco [24] established a link between the stoichiometric coefficient of the hydrocracking reactions and the parameters P_{ij} of Stangeland's kinetic model; this analogy imposes a constraint on the values that the P_{ij} matrix can take. Such a constraint is given by the mass balance closure in each of the hydrocracking reactions and would require the determination of the values of the parameters B and C (Table 9). It was noticed that only with these two parameters is not possible to rearrange the product distribution to satisfy the mass balance for each individual reaction.

These authors modified the model proposed by Stangeland by adding two additional parameters, B_2 and ω as shown in Table 9, so that the mass balance in each individual hydrocracking reaction is satisfied. They used a second-order hydrocracking rate constant to quantify the effect of hydrogen partial pressure on the rate of cracking. The kinetic constants are determined from the pseudo-first-order constants reported by Qader and Hill [8]. This model was applied to the hydrocracking of VGO in a commercial reactor described by Mohanty et al. [23].

2.2. Models based on continuous mixtures

Laxminarasimham et al. [25] developed a kinetic model for hydrocracking of a petroleum mixture based on the continuous theory of lumping. The model considers properties of the reaction mixture, the underlying pathways, and the associated selectivity of the reactions. The parameter of characterization is the true boiling point temperature (TBP). During the reaction of a particular feed, the mixture's distillation curve changes continuously inside the reactor, and as the residence time increases, most of the heavier components are converted into lighter components. A normalized TBP as a function of an index (θ) is used instead of the TBP. Normalized TBP is defined by Eq. (21). The reactivity is considered to be monotonic and can be represented by a simple power law type function [Eq. (22)], where k is the reaction rate of a particular compound,

k_{max} is the reaction rate of the compound of higher TBP, and α is a model parameter. The model equations are formulated as a function of reactivity following the procedure proposed by Chou and Ho [26]. In order to express the equation with k as the independent reactivity, a transformation operator is required, which is approximated by Eq. (23). $D(k)$ can be considered as a species-type distribution function, where N is the number of compounds in the mixture and tends toward infinitum in a heavy fraction of oil:

$$\theta = \frac{\mathrm{TBP} - \mathrm{TBP}(l)}{\mathrm{TBP}(h) - \mathrm{TBP}(l)} \tag{21}$$

$$\frac{k}{k_{max}} = \theta^{1/\alpha} \tag{22}$$

$$D(k) = \frac{N\alpha}{k_{max}^{\alpha}} k^{\alpha-1} \tag{23}$$

A material balance of species of reactivity k, the core of the kinetic model, can be expressed with an integrodifferential equation:

$$\frac{\mathrm{d}C(k,t)}{\mathrm{d}t} = -kC(k,t) + \int_k^{k_{max}} [p(k,K)KC(K,t)D(K)]\,\mathrm{d}K \tag{24}$$

$p(k, K)$ is ideally the yield distribution function that describes the formation of compounds of reactivity k from hydrocracking of compounds of reactivity K. This function is approximated in this model by a skewed Gaussian-type distribution function obtained from experimental data on the reactivity of several model compounds [Eqs. (25)–(28)]. The parameters a_0, a_1, and δ are specific for each system and are used for model tuning:

$$p(k,K) = \frac{1}{\mathrm{So}\sqrt{2\pi}} \left\{ \exp\left[-\left(\frac{(k/K)^{a_0} - 0.5}{a_1} \right)^2 \right] - A + B \right\} \tag{25}$$

$$A = e^{-(0.5/a_1)^2} \tag{26}$$

$$B = \delta\left(1 - \frac{k}{K}\right) \tag{27}$$

$$\mathrm{So} = \int_0^K \frac{1}{\sqrt{2\pi}} \times \left\{ \exp\left[-\left(\frac{(k/K)^{a_0} - 0.5}{a_1} \right)^2 \right] - A + B \right\} D(K)\,\mathrm{d}k \tag{28}$$

This model was successfully applied to experimental data previously published [21,27]. Bennett and Bourne [21] reported product yields from the hydrocracking of Kuwait vacuum gas oil at four different residence times: 0.383, 0.952, 1.724, and 2.5 h. The set of parameters was tuned using data obtained at 2.5 h of residence time. These parameters are: $\alpha = 1.35$, $k_{max} = 1.35\ \mathrm{h}^{-1}$, $a_0 = 6.41$, $a_1 = 28.15$, and $\delta = 2.6667 \times 10^{-5}$. Fig. 14 shows a typical $p(k, K)$ function, in this case, $k = k_{max}$. Comparisons of experimental and estimated values are shown in Fig. 15 and in Table 11.

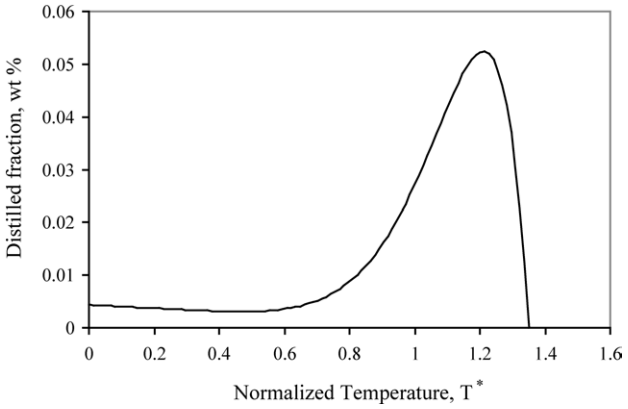

Fig. 14. Yield distribution function $p(k, K)$ for Bennet and Bourne [21] experimental data.

El-Kady [27] reported another set of experimental data at several reaction temperatures and residence times for the hydrocracking of a vacuum gasoil. In Fig. 16 and Table 12, comparisons of these experimental data and estimated values at 390°C are presented. The set of fitted parameters of the model reported by Laxminarasimhan et al. [25] is: $\alpha = 0.77$, $k_{max} = 0.88\ \mathrm{h}^{-1}$, $a_0 = 3.67$, $a_1 = 22.86$, and $\delta = 0.77 \times 10^{-9}$ for experimental data at 390 °C.

Extensions of the Laxminarasimhan et al. model [25], in which the reacting mixture is divided into continuous mixtures of paraffinic, naphthenic, and aromatics components, have been published by the same research group [28,29]. In addition to the reactions of hydrocracking that form compounds on the same family, the formation reactions of paraffins from naphthenes, paraffins from aromatics, and naphthenes from aromatics were considered. Therefore, the models require the definition of a concentration function, a reactivity function, and a species

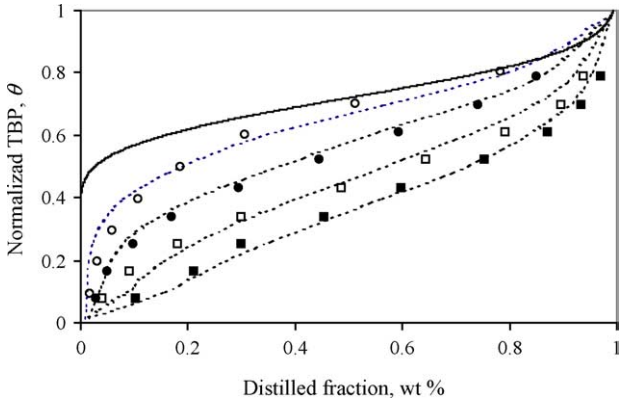

Fig. 15. Comparison of estimations (- - -) with Laxminarasimhan et al. model [25] and experimental results of Bennett and Bourne [21]: (—) feed; (○) 0.383 h; (●) 0.952 h; (□) 1.724 h; (■) 2.5 h.

Table 11
Comparison of experimental data reported by Bennett and Bourne [21] with those predicted by Laxminarasimhan et al. model [25]

Residence time (h)	Feed	0.383	0.952	1.724	2.5
Gasoline (30–150 °C)					
Experimental (wt.%)	0.0	6	16.0	23.0	26.0
Predicted (wt.%)	–	5.5	16.0	21.0	25.0
Absolute difference (wt.%)		1.5	0.0	2.0	1.0
Error (%)		8.3	0.0	8.7	3.8
Middle distillates (150–370 °C)					
Experimental (wt.%)	41.0	45.0	51.0	61.0	39.0
Predicted (wt.%)	–	52.0	53.0	59.0	35.0
Absolute difference (wt.%)		7.0	2.0	2.0	4.0
Error (%)		−15.6	−3.9	3.3	10.3
370 °C+					
Experimental (wt.%)	59.0	35.0	25.0	9.0	5.0
Predicted (wt.%)	–	40.0	25.0	11.0	7.5
Absolute difference (wt.%)		5.0	0.0	2.0	2.5
Error (%)		−14.3	0.0	−22.2	−50.0

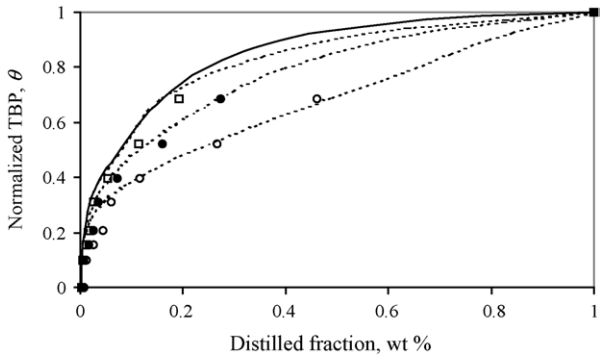

Fig. 16. Comparison of estimations (- - -) with Laxminarasimhan et al. model [25] and experimental data of El-Kady [27]: (—) feed; (○) 1.5 h; (●) 1.0 h; (□) 0.667 h residence time.

Table 12
Comparison of experimental data reported by El-Kady [27] with those predicted by Laxminarasimhan et al. model [25]

Residence time (h)	Feed	0.667	1	2
Gasoline (30–150 °C)				
Experimental (wt.%)	3.0	3.01	5.0	7.5
Predicted (wt.%)	–	3.25	5.0	6.0
Absolute difference (wt.%)		0.24	0.0	1.5
Error (%)		−8.0	0.0	20.0
Middle distillate (150–370 °C)				
Experimental (wt.%)	13.5	14.0	23.0	36.0
Predicted (wt.%)	–	13.9	24.0	39.0
Absolute difference (wt.%)		0.1	1.0	3.0
Error (%)		0.7	−4.3	−8.3
370 °C+				
Experimental (wt.%)	82.5	80.0	70.0	54.0
Predicted (wt.%)	–	79.6	70.0	51.0
Absolute difference (wt.%)		0.4	0.0	3.0
Error (%)		0.5	0.0	5.6

distribution function for each family of compounds, as well as six different product distribution functions. The models were validated with the pilot plant experimental data reported by Bennett and Bourne [21]. However, parameters of the model functions were not reported.

2.3. Structure oriented lumping and single event models

Structure oriented lumping kinetic models, which employ most of the information obtained with the modern analytical techniques for model reaction modeling at a molecular level, have been proposed for some catalytic processes. The lumps are defined according to the structure of the compounds in the reacting mixture.

Liguras and Allen [30] utilized contribution group concepts, which provide a mechanism for making use of pure compound data in modeling complex reactions. They describe the conversion of vacuum gas oil in terms of a relatively large number of pseudo-components, most of which are lumps in their own right. Quann and Jaffe [31,32] developed a procedure to describe molecules and reactions with a notation of vectors, which allows a computer program to represent the reaction networks. These authors expressed the chemical transformations in terms of a typical structure of the molecules without completely eliminating lumps and rate parameters that depend on the feedstock composition.

Martens and Marin [33] reported a model for the hydrocracking of hydrogenated vacuum gas oil based on theoretical and mechanistic considerations. The reaction mechanism is described by a set of single events, each of which can be ascribed a rate equation or a term in a single rate equation. The model considers the reaction rules for the carbenium ion of the secondary and tertiary types. A computer algorithm was used for generating the reaction networks.

Froment [34] has recently reviewed the single event approach, which retains the full detail of the reaction pathways of the individual feed components and reaction intermediates. This approach is illustrated by means of the methanol-to-olefins and catalytic cracking of oil fractions reactions. It is also highlighted that other important processes with complex feedstocks, such as catalytic reforming, hydrocracking, alkylation, and isomerization, can be modeled with the single event concept.

As can be seen, all these approaches have been successfully applied for some complex reaction systems. Other applications to kinetic modeling of pure compounds conversion have also been reported, which is not the main subject of the present review. However, hydrocracking kinetics of oil fractions with structure oriented lumping modeling or the single event approach have not been reported in the open literature. Froment, in his review [34], has mentioned the application of single event kinetic modeling to the hydrocracking of vacuum gas oil with a complication due to the multiphase operation of hydrocrackers, but the paper has not yet been published [35].

3. Comparison of kinetics models

In this section, we present a comparison of various kinetic models for hydrocracking of heavy oils in order to identify and

establish their capabilities and accuracy in the prediction of conversion and product yields. One representative model of each of the already described models was selected; these are summarized as follows:

- Model 1. The oldest kinetic model for hydrocracking of heavy oils that only includes the feed conversion according to the following reaction scheme [8]:

$$\text{feed}(A) \xrightarrow{k_0} \text{products}$$

$$(r_A) = -k_0 y_A \quad (29)$$

- Model 2. The three-lump kinetic model reported by Callejas and Martínez [9] that splits the products lump into light oils and gases:

$$\text{feed}(A) \xrightarrow{k_1} \text{light oils}(B), \qquad \text{feed}(A) \xrightarrow{k_2} \text{gases}(C)$$

$$(r_A) = -(k_1 + k_2) y_A = -k_0 y_A \quad (30)$$

$$(r_B) = k_1 y_A \quad (31)$$

$$(r_C) = k_2 y_A \quad (32)$$

- Model 3. The model proposed by Stangeland [22] was chosen to represent the family of models based on pseudo-components, which offer more information about the composition of reaction products. The main equations for this model, which involve four parameters (k_0, A, B, C), were given in Table 9.
- Model 4. The model based on continuous mixtures reported by Laxminararshmhan et al. [25], which uses TBP temperature data as a characterization parameter. The general model is represented by Eqs. (21)–(28). These equations involve two parameters to be estimated, k_{max} and α. The values of the other parameters (a_0, a_1, and δ) were assumed to be those reported in [25].

The experimental data used for parameter estimation of the four models were taken from the literature [27], in which hydrocracking of vacuum gas oil was carried out in an isothermal plug flow reactor within a wide range of operating conditions: reaction temperatures of 390, 410, 430, and 450 °C; LHSV of 0.5, 1.0, 1.5, 2.0, and 2.5 h^{-1} at constant pressure of 10.34 MPa; a hydrogen-to-oil ratio of 1000 Std m^3/m^3. The reaction was conducted using a bifunctional molybdenum–nickel over silica–alumina catalyst, which was replaced by fresh catalyst after a few operations. With catalyst replacement, the authors were assured it works in a regime in which catalyst deactivation can be neglected. Liquid product was distilled into light naphtha (IBP-80 °C), gasoline (80–150 °C), kerosene (150–250 °C), gas oil (250–380 °C), and residue (380 °C+). It should be mentioned that this paper reported very detailed experimental information and several researchers have used these data for testing kinetic models.

With the experimental data and the four selected kinetic models, the best sets of kinetic parameters were obtained with a non-linear regression procedure based on the Levenberg–Marquardt method [36]. This was accomplished by minimizing the objective function based on the sum of square errors between experimental and calculated product yields.

Table 13
Kinetic parameters obtained for different models

	Temperature (°C)				E_A (kcal/mol)
	390	410	430	450	
Model 1					
k_0 (h^{-1})	0.3147	0.5377	0.9206	1.8264	27.63
Model 2					
k_1 (h^{-1})	0.2768	0.4692	0.7768	1.5194	26.69
k_2 (h^{-1})	0.0379	0.0685	0.1438	0.3070	33.35
k_3 (h^{-1})	0.0167	0.0405	0.0933	0.2055	39.88
Model 3					
k_0	0.6472	1.1469	1.9018	3.2086	25.29
A	1.0000	1.0000	1.0000	0.7558	
B	0.6463	0.5506	0.3722	−0.4278	
C	1.0671	0.6559	0.6996	0.3567	
Model 4					
k_{max} (h^{-1})	0.6030	1.1423	2.1058	3.6967	28.84
α	1.0724	0.8936	0.7671	0.8264	

Table 13 summarizes the values of kinetic parameters from the different models. If we observe the values of k_0 from Model 1, and k_1 and k_2 from Model 2, we can conclude that the condition $k_0 = k_1 + k_2$ is satisfied. This means that both models are essentially the same with the advantage that Model 2 can predict light oil and gases yields separately. Therefore, only Model 2 will be compared with the other two models.

As expected, the activation energy of the overall hydrocracking (E_{A0}) is between E_{A1} and E_{A2}. Of course, the value of E_{A0} is closer to E_{A1} since k_1 is also much closer to k_0.

The error in predictions of product yields with Model 2 is quite acceptable at temperatures of 390, 410, and 430 °C; however, at 450 °C the error is higher, as can be seen in Fig. 17. One reason for this could be the fact that at high temperatures the selectivity of the reaction changes substantially and light oils may start forming gases. This can be possible if we remember that the feed for these experiments is relatively light (vacuum gas oil) as compared with typical feed for the hydrocracking process, e.g., petroleum residua. To confirm this, we included a new path reaction in Model 2 (light oils $\xrightarrow{k_3}$ gases) with an additional kinetic constant, k_3. A comparison of predicted middle distillates and gas yields with experimental data with and without k_3 is

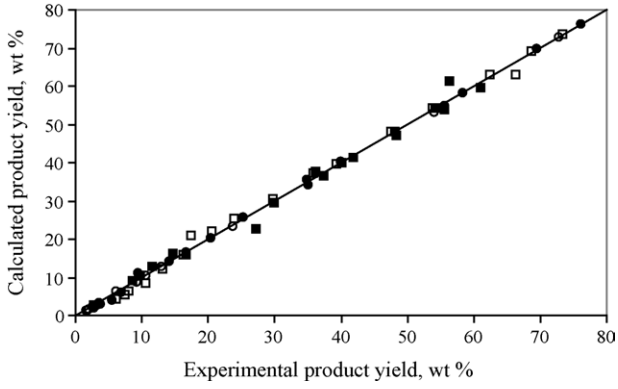

Fig. 17. Comparison of experimental data [27] and results of Model 2 [9]: (○) 390 °C; (●) 410 °C; (□) 430 °C; (■) 450 °C.

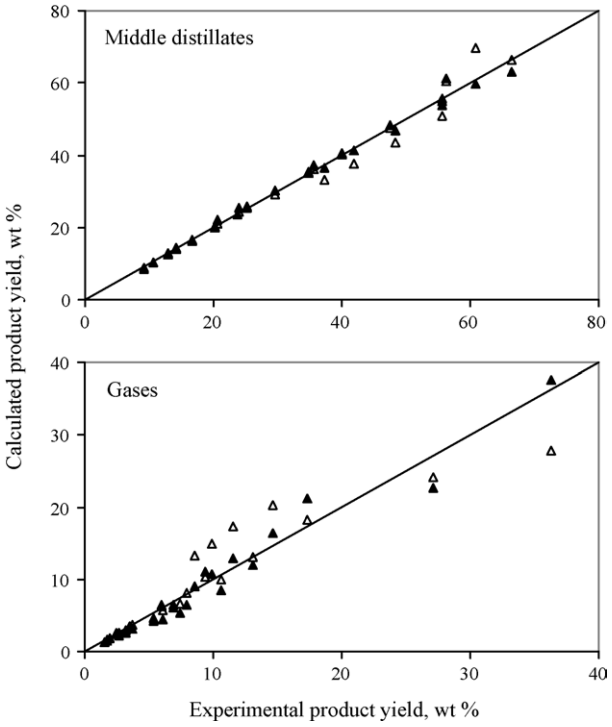

Fig. 18. Comparison of experimental [27] and calculated yields using the kinetic scheme shown in Fig. 1b [9]: with k_3 (full symbols) and without k_3 (void symbols).

shown in Fig. 18. The average absolute error is lower when k_3 is incorporated into the model. This indicates that gas formation from light oils should be included in this kinetic model.

After observing this, we went back to the experimental data and kinetic parameters reported by Callejas and Martínez [9], which were discussed in Section 2.1.1, and we tried to determine k_3, but the estimation always gave zero as the best adjusted value. This can be due either to the insufficient experimental data or to the low probability of gas formation from light oils in that type of feed (residue) at the reaction conditions of such a study.

From these results one main conclusion can be established: simple lumped kinetic models are useful for predicting hydrocracking reaction behavior within a reduced range of operating conditions, depending on the type of feedstock. That could be the reason why some authors calculate kinetic parameters applying lumped models for different reaction temperature regimes [14].

As for Models 3 and 4, kinetic parameters are also reported in Table 13. k_0 of Model 3 and k_{max} of Model 4 increase with temperature, and hence, activation energies were calculated. The values of E_A with these two parameters are very close to the activation energy found for Model 1 (and 2) for total feed conversion. Therefore, k_0 and k_{max} do indeed represent kinetic parameters, although the authors do not mention this clearly.

When optimizing the parameter values of Model 3, the best solution was found with $A > 1.0$; however, as the authors stated, A must be in the range of -1.0 to 1.0, and preferably from 0 to 1.0. This constraint was added to the optimization program, after which the best solution obtained was with

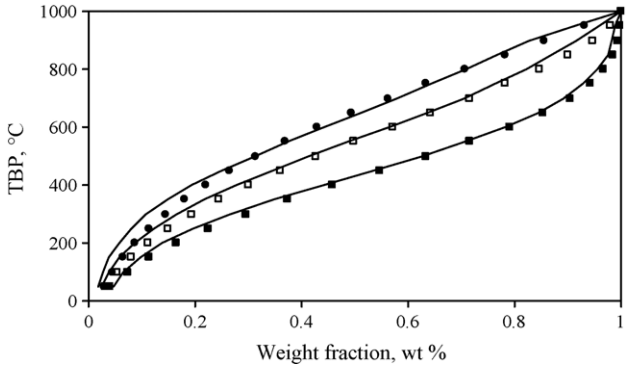

Fig. 19. Comparison of experimental (symbols) and calculated (lines) results of the kinetic model proposed by Stangeland [22] using reported data [27] at temperature of 430 °C: (●) LHSV = 1.5 h^{-1}; (□) LHSV = 1.0 h^{-1}; (■) LHSV = 0.5 h^{-1}.

$A = 1.0$, except at 450 °C ($A = 0.7558$). Predictions with $A > 1.0$ and $0 \leq A \leq 1.0$ were not very different. Fig. 19 shows calculated and experimental TBP distillation curves for hydrocracked products at different LHSV. It is observed that predicted distillation curves are very close to those reported experimentally.

For Model 4, Laxminarasimhan et al. [25] reported values of $k_{max} = 0.88$ and $\alpha = 0.77$ for the same experimental data [27] at 390 °C, which differ from our results at the same temperature ($k_{max} = 0.6030$ and $\alpha = 1.0724$). For parameter estimation, the authors mentioned that they did not use experimental data at all LHSV, but only at LHSV = 0.5 h^{-1}. Thus, our parameter values considering all LHSV better represent the experiments and are presented in Table 13. The comparison of experimental and calculated normalized TBP distillation curves reported by Laxminarasimhan et al. [25] at 390 °C is shown in Fig. 16. It was observed that predictions at low LHSV are better than at high LHSV, which is due, in part, to the use of only one LHSV value for determining k_{max} and α. For our parameter values, this comparison is presented in Fig. 20 at the same temperature (390 °C). The slightly better agreement of experimental and calculated normalized TBP distillation curves compared with the predictions of Laxminarasimhan et al. [25] may not be clearly seen. However, if we observe Fig. 16 again (with the

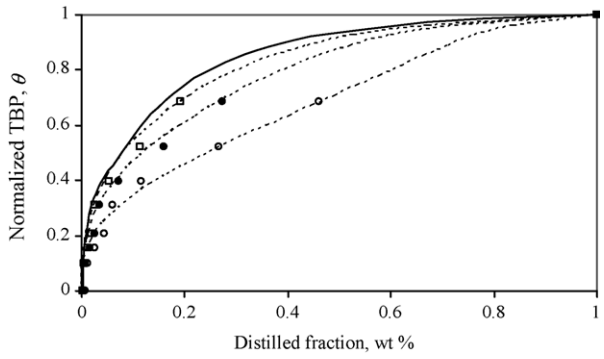

Fig. 20. Comparison of estimations (- - -) with Laxminarasimhan et al. model [25] with parameter estimation of this work and experimental data of El-Kady [27]: (—) feed; (○) 1.5 h; (●) 1.0 h; (□) 0.667 h residence time.

Table 14
Activation energies reported in the literature for experiments of hydrocracking of petroleum fractions

Reference	Feed	Reactor type	Catalyst	P (MPa)	T (°C)	LHSV (h^{-1})	H_2/oil (m^3/m^3)	Activation energy (kcal/mol)				
								Feed conversion	Gas formation	Gasoline formation	MD formation	Naphtha from MD
[8]	GO	TBR	NiW/SiO_2–Al_2O_3	10.34	400–500	0.5–3.0	500	21.1	–	–	–	–
[9]	AR	CSTR	$NiMo/Al_2O_3$	12.5	375–415	1.4–7.1	–	41.3[a]	43.9[a]	–	–	–
[10]	VGO	TBR	NiMo-HY/SiO_2–Al_2O_3	12	400–450	0.5–2.0	–	17–22.5[a]	18.6–18.9	22.2–24.0	13.0–17.5	–
[11]	GO	TBR	$NiMo/Al_2O_3$	7–11	350–400	0.7–1.5	600	17.2–17.7	–	29.7–32.1	14.3–15.0	20.5–26.9
[12]	VGO	TBR	$CoMo/Al_2O_3$	5.0–10.1	400–450	–	–	53.2–66.6	–	–	–	–
[14]	HGO	TBR	$NiMo/Al_2O_3$	8.8	340–420	1.0	600	24.1–33.2	–	–	28.4	8.8–31.8
[19]	HO	TBR	$NiMo/Al_2O_3$	6.9	380–420	0.33–1.5	890	27.3–48.5	27.3	38.0	39.5	53.7

[a] Values recalculated in this work.

original parameter values) with more detail, we see that at 0.667 h residence time the hydrocracked product's predicted distillation curve in the range of 0–20 wt.% overlaps, and in some parts is slightly above the feed distillation curve. This does not happen with our predictions, which are closer to experimental values (Fig. 20). The reason for this discrepancy is clearly due to the use of only LHSV = 0.5 h^{-1} (2.0 h residence time) by Laxminarasimhan et al. [25], while we have employed all LHSV experimental data to determine optimal parameter values.

A summary of reaction conditions and activation energies found in the literature for hydrocracking experiments is presented in Table 14. It is seen that E_A values obtained in this work are within the range of those reported by others. The higher activation energies of some hydrocracking reactions indicate high temperature sensitivity for those reactions. For instance, activation energy for naphtha formation from middle distillates is higher than that of formation of heavy products, indicating higher temperature sensitivity for this reaction. This means that an increase in temperature will also increase naphtha production more than the production of other products. Another observation from this table is that for similar reaction conditions and catalyst, the heavier the feed, the higher the activation energy, which is also in line with the behavior found for other hydroprocessing reactions [37]. Also, the different catalyst composition (e.g. support, promoter, etc.) evidences the role played by catalyst properties in reaction selectivity.

To compare model predictions with experimental data, it was necessary to group products into gases, gasoline plus middle distillates (IBP-380 °C), and unconverted residue (380 °C+). For Models 1 and 2 this was done directly, but for Models 3 and 4 product yield values were determined with predicted distillation curves.

Table 15
Comparison of different kinetics models with data experimental reported by El-Kady [27] at 390 °C, 10 MPa and 1.0 h^{-1} LHSV

	Experimental	Model 1	Model 2	Model 3	Model 4
Gases	2.46	26.08	2.64	1.42[a]	1.17
Gasoline + MD[b]	24.77		23.44	28.48	24.92
Residue[c]	72.77	72.98	72.98	70.10	73.91

[a] C_1–C_3 fraction is not included.
[b] IBP-380 °C.
[c] 380 °C+.

A comparison of experimental and calculated yields with the four models is presented in Table 15. Model 1 is only capable of predicting gases and gasoline + MD yields together, while the other models can predict these lumps separately. Models 1 and 2 predicted product yields with very low error, while Models 3 and 4 underestimated gas yield, but determined residue and middle distillate yields with reasonable accuracy.

The huge advantage of Models 3 and 4 against Models 1 and 2 is that they can predict not only these lumps, but also the entire distillation curve of the product, and hence any product yield can be calculated by specifying only distillation ranges. On the other hand, parameter estimation for Models 1 and 2 is quite easy, while parameter estimation for Models 3 and 4 is much more complicated. The data required in Models 1 and 2 (product yields) are also easy to obtain from mass balances during the reaction, while Models 3 and 4 require additional characterization of the products, e.g., the TBP distillation curve.

As can be seen, the approaches for kinetic modeling of heavy oils hydrocracking reported in the literature have different capabilities. Product yield prediction is quite similar, which, of course, depends on the quality of experimental data and robustness of the parameter optimization method. Parameter estimation for lump models is not difficult; however, when the number of lumps is increased, it could sometimes become difficult to find the optimal solution. To reduce complexity, the use of sequential estimation of parameters is an option, since parameter values obtained with a few lumps can be employed as an initial guess for more lump models. This approach has been successfully applied to parameter estimation for other catalytic reactions [38,39].

4. Conclusions

Lump models have been used for several years for kinetic modeling of complex reactions. In fact, some commercial catalytic process design is still being performed with this type of approach. Catalyst screening, process control, basic process studies, and dynamic modeling, among others, are areas in which lump kinetic models are extensively applied. The main disadvantages of lump models are their simplicity in predicting product yields, the dependency of kinetic parameters on feed properties, and the use of an invariant distillation range of

products, which, if changed, necessitates further experiments and parameter estimation.

Models based on continuous mixtures (continuous theory of lumping) overcome some of these deficiencies by considering properties of the reaction mixture, the underlying pathways, and the associated selectivity of the reactions. The common parameter of characterization is the true boiling point temperature, since during reaction it changes continuously inside the reactor as the residence time increases. However, dependency of model parameters on feed properties is still present. Distillation curves, either chromatographic or physical, also present some difficulties when analyzing heavy oils since initial and final boiling points are not accurate during experimentation. In fact, for many purposes, 10% and 90% boiling point are commonly utilized instead of IBP and FBP, respectively.

Structure oriented lumping models are more detailed approaches that express the chemical transformations in terms of typical molecule structures. These models describe reaction kinetics in terms of a relatively large number of pseudocomponents, and hence they do not completely eliminate lumps. In addition, dependency of rate parameters on feed properties is present.

The single event concept uses elementary steps of cation chemistry, which consists of a limited number of types of steps involving series of homologous species. The number of rate coefficients to be determined from experimental information can be reduced and are modeled based upon transition state theory and statistical thermodynamics. With this approach, parameter values are not dependent on feed properties. However, even though the number of parameters can be diminished, detailed and sufficient experimental data are necessary.

The complexity of real feedstocks suggests that models based on lumping theory will continue to be used for the study of hydrocracking reaction kinetics. However, more sophisticated and accurate approaches need to be studied with more detail for a better understanding and representation of heavy oil hydrocracking kinetics.

Acknowledgment

The authors thank the Instituto Mexicano del Petróleo for financial support. M.A. Rodríguez also thanks the CONACyT for financial support.

References

[1] J. Scherzer, A.J. Gruia, Hydrocracking Science and Technology, Marcel Dekker, 1996.
[2] G.F. Froment, K.B. Bischoff, Chemical Reactor Analysis and Design, 2nd ed., John Wiley & Sons, 1990.
[3] J. Wei, J.C.W. Kuo, Ind. Eng. Chem. Res. 8 (1969) 114.
[4] N. Choudhary, D.N. Saraf, Ind. Eng. Chem. Prod. Res. Dev. 14 (1975) 74–83.
[5] S. Mohanty, D. Kunzru, D.N. Saraf, Fuel 69 (1990) 1467–1473.
[6] U. Chaudhuri, U.R. Chaudhuri, S. Datta, S.K. Sanyal, Fuel Sci. Technol. Int. 13 (1995) 1199–1213.
[7] G. Valavarasu, M. Bhaskar, K.S. Balarman, Petrol. Sci. Technol. 21 (2003) 1185–1205.
[8] S.A. Qader, G.R. Hill, Ind. Eng. Chem. Process Des. Dev. 8 (1969) 98–105.
[9] M.A. Callejas, M.T. Martínez, Ind. Eng. Chem. Res. 38 (1999) 3285–3289.
[10] K. Aboul-Gheit, Erdoel Erdgas Kohle 105 (1989) 319–320.
[11] S.M. Yui, E.C. Sanford, Ind. Eng. Chem. Res. 28 (1989) 1278–1284.
[12] D.I. Orochko, Khimiya I Tekhnologiya Topliv i Masel 8 (1970) 2–6.
[13] Y. Perezhigina, A.V. Agafonov, M.V. Rysakov, S.P. Rogov, TsNIITÉ Neftekhim (1968) 59.
[14] C. Botchwey, A.K. Dalai, J. Adjaye, Can. J. Chem. Eng. 82 (2004) 478–487.
[15] C. Botchwey, A.K. Dalai, J. Adjaye, Energy Fuels 17 (2003) 1372–1381.
[16] K. Aoyagi, W.C. McCaffrey, M.R. Gray, Petrol. Sci. Technol. 21 (2003) 997–1015.
[17] F. Mosby, R.D. Buttke, J.A. Cox, C. Nikolaides, Chem. Eng. Sci. 41 (1986) 989.
[18] R. Ayasse, H. Nagaishi, E.W. Chan, M.R. Gray, Fuel 76 (1997) 1025–1033.
[19] S. Sánchez, M.A. Rodríguez, J. Ancheyta, Kinetic model for moderate hydrocracking of heavy oils, Ind. Eng. Chem. Res., in press.
[20] R. Krishna, A.K. Saxena, Chem. Eng. Sci. 44 (1989) 703–712.
[21] R.N. Bennett, K.H. Bourne, in: Proceedings of the ACS Symposium On Advances in Distillate and Residual Oil Technology, New York, 1972.
[22] B.E. Stangeland, Ind. Eng. Chem. Process. Des. Dev. 13 (1974) 71–75.
[23] S. Mohanty, D.N. Saraf, D. Kunzru, Fuel Process Technol. 29 (1991) 1–17.
[24] C.G. Dassori, M.A. Pacheco, Chem. Eng. Commun. 189 (2002) 1684–1704.
[25] C.S. Laxminarasimhan, R.P. Verma, AIChE J. 42 (1996) 2645–2653.
[26] Y. Chou, T.C. Ho, AIChE J. 35 (1989) 533.
[27] F.Y. El-Kady, Indian J. Technol. 17 (1979) 176.
[28] C.S.L. Narasimhan, M. Sau, R.P. Verma, Stud. Surf. Sci. Catal., vol. 127, Elsevier Science, 1999.
[29] K. Basak, M. Sau, U. Manna, R.P. Verma, Catal. Today 98 (2004) 253–264.
[30] D.K. Liguras, D.T. Allen, Ind. Eng. Chem. Res. 28 (1989) 665–673.
[31] R.J. Quann, S.B. Jaffe, Ind. Eng. Chem. Res. 31 (1992) 2483–2497.
[32] R.J. Quann, S.B. Jaffe, Chem. Eng. Sci. 31 (1996) 1615.
[33] G.G. Martens, G.B. Marin, AIChE J. 47 (2001) 1607–1622.
[34] G.F. Froment, Catal. Rev. Sci. Eng. 47 (2005) 83–124.
[35] J. Govindakannan, G.F. Froment, in press.
[36] D. Marquardt, J. Soc. Ind. Appl. Math. 11 (1963) 431.
[37] J. Ancheyta, M.J. Angeles, M.J. Macías, G. Marroquín, R. Morales, Energy Fuels 16 (2002) 189–193.
[38] J. Ancheyta, F. López, E. Aguilar, J.C. Moreno, Ind. Eng. Chem. Res. 36 (1997) 5170–5174.
[39] J. Ancheyta, R. Sotelo, Energy Fuels 14 (2000) 1226–1231.